ELECTRON INTERBAND TRANSITIONS IN NICKEL

M. M. KIRILLOVA

Institute of Metal Physics, USSR Academy of Sciences

Submitted February 2, 1971

Zh. Eksp. Teor. Fiz. **61**, 336—344 (July, 1971)

The frequency dispersion of the dielectric constant $\epsilon(\omega)$ of Ni (110) and Ni (100) single-crystal samples is measured in the 0.265—20-micron (4.9—0.06 eV) spectral range. Some features of the interband transitions are studied. The results are discussed on basis of modern concepts regarding the structure of the energy spectrum of nickel.

THE electronic structure of nickel has been the subject of intense studies in recent years. Theoretical calculations of the band spectrum[1,2] and experimental investigations have led to the development of a number of models of the energy bands of ferromagnetic nickel[3-6], which explain with different degrees of success the data on the de Haas—van Alphen effect, magnetoresistance, electronic specific heat, the ferromagnetic Kerr effect, etc.

During the course of development of the models, the main discussion was concentrated on the question of the mutual placement of the L_{32} and $L_{2'}$ levels and the Fermi level. Definite interest was therefore aroused by optical and magnetooptical measurements in nickel in the near infrared region, since it is precisely these data that can yield quantitative information on the spin-orbit and exchange splitting of the bands near the Fermi level.

Optical measurements performed on polycrystalline samples in the infrared region of the spectrum revealed interband transitions at energies 0.3 and 1.3—1.4 eV[3,7]. More detailed measurements performed in[8], also on a polycrystalline nickel sample, revealed additional singularities on the $\sigma(\omega)$ curve (ω—cyclic frequency of the light wave), mostly in the form of very weak bursts. It is to be expected that the fine details in the absorption spectrum of nickel, connected with interband transitions, will be more clearly pronounced when the measurements are made on single crystals. We have investigated in detail the optical properties of single-crystal nickel samples in the broad spectral interval 0.265—20 μ. Particular attention was paid to a study of the fine structure on the conductivity curve $\sigma(\omega)$, connected with the interband transitions. The results are discussed on the basis of the band model proposed in[5,6,9] for nickel.

SAMPLES, MEASUREMENT METHOD, RESULTS

The samples were cut from nickel single crystals grown by the Czochralski method. The crystals were cut by the electric-spark method along the (110) and (100) planes. The accuracy of the face orientation, $\pm 2°$, was monitored by the Laue back-reflection method. The surfaces of samples measuring 20 × 70 mm were ground with different powders, and then polished with an electrolyte having the following composition: H_2SO_4 (910 g/liter), H_3PO_4 (750 g/liter), citric acid (20 g/liter) and H_2O (40 ml). The cathode was lead and the anodic current density was j = 0.4 A/cm^2. The long distance between the electrodes ($\sim$120 mm) and proper

screening of the sample ensured a sufficiently uniform material removal from the entire surface of the crystal. The optimum electrolyte temperature at which a smooth surface without relief was obtained was 5—10°C.

X-ray-diffraction and optical investigations have shown that to rid the sample surface of the cold-working layer it is necessary to remove 150—180 μ. The amount of material removed was determined by experiment. Topograms of crystals with removed layers of 50, 100, 150 and 200 μ were obtained by the Schultz method in white light, and have shown that the stresses are eliminated from the sample only if a layer of $\sim$150 μ is removed. We measured ψ and Δ simultaneously (ψ—azimuth of the "reconstructed" polarization and Δ is the difference between the phase discontinuities of the s and p components of the reflected light); their values were stabilized when a layer of $\sim$150 μ was removed. Figure 1 shows the variation of the quantity $2\pi\sigma(\omega)$ = nkω in the visible and ultraviolet regions of the spectrum as functions of the amount of material removed. It is noted also that 2—3 hours after the polishing, the values of ψ decreased and those of Δ increased, apparently as a result of formation of an oxide film on the surface of the sample. To eliminate the influence of the oxide film, the optical measurements were performed during the first 2—3 hours after polishing. Further measurements were made only after electrically polishing the sample again for five minutes.

The refractive index n and the absorption coefficient k were measured by the Beattie polarometric method[10], using an IKS-12 infrared spectrometer and an SF-4 spectrophotometer. Fourfold reflection of light from the samples was used in the infrared region, and single
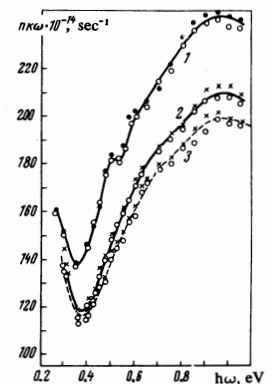

FIG. 1. Effect of the thickness of metal removed by electric polishing on the quantity $2\pi\sigma$ = nkω. Curve 1: O—removed layer 200μ, ●—105μ (for Ni (110)); curve 2—removed layer 80μ, O—for Ni (110), X—for Ni (100); curve 3—removed layer 40μ, O—for Ni (110), X—for Ni (100).

Table I

λ, μ	n	k	λ, μ	n	k	λ, μ	n	k
0.265	1.20	2.19	1.25	2.86	6.08	4.4	4.90	16.0
0.280	1.30	2.12	1.30	3.00	6.13	4.5	4.88	16.3
0.288	1.30	2.08	1.35	3.07	6.42	5.0	4.95	18.5
0.302	1.30	2.07	1.45	3.15	6.87	5.25	4.80	19.1
0.312	1.28	2.05	1.50	3.10	7.05	5.50	4.90	20.0
0.365	1.20	2.31	1.60	3.25	7.12	5.75	5.26	21.8
0.400	1.20	2.51	1.65	3.48	7.42	6.25	5.15	23.0
0.425	1.25	2.71	1.70	3.45	7.63	6.50	5.40	24.6
0.450	1.37	2.90	1.75	3.54	7.70	6.75	5.65	25.8
0.460	1.44	2.96	1.80	3.53	8.10	7.00	5.80	26.8
0.470	1.46	2.98	1.90	3.63	8.48	7.25	6.10	27.8
0.480	1.47	3.04	2.0	3.62	8.55	7.50	6.20	28.8
0.490	1.50	3.08	2.1	3.72	8.96	7.75	6.27	29.5
0.500	1.54	3.10	2.2	3.95	9.28	8.00	6.20	30.3
0.510	1.56	3.16	2.3	3.88	9.80	8.25	6.40	31.2
0.520	1.60	3.22	2.4	3.80	10.1	8.50	6.65	32.0
0.530	1.65	3.23	2.5	3.90	10.4	8.75	7.35	32.4
0.540	1.64	3.28	2.6	4.13	10.7	9.00	7.30	33.5
0.550	1.67	3.40	2.7	4.20	11.9	9.50	7.05	35.1
0.575	1.68	3.53	2.8	4.22	12.0	10.0	8.22	36.0
0.600	1.74	3.68	2.9	4.50	11.9	10.5	8.50	37.7
0.650	1.82	3.90	3.0	4.53	12.3	11.0	8.50	39.4
0.700	1.88	4.19	3.1	4.53	12.4	11.5	8.80	40.6
0.750	2.00	4.40	3.2	4.59	12.7	12.0	9.00	42.0
0.800	2.18	4.56	3.3	4.70	12.6	12.5	9.54	42.6
0.850	2.29	4.73	3.4	4.72	13.0	13.0	9.90	44.1
0.900	2.36	4.90	3.6	4.82	13.6	14.0	10.8	46.7
0.950	2.44	5.15	3.7	5.05	14.2	15.0	11.2	48.2
1.00	2.52	5.20	3.8	5.30	14.2	16.0	12.0	50.3
1.10	2.65	5.50	3.9	5.13	14.5	17.0	12.5	52.0
1.15	2.80	5.80	4.0	5.04	15.1	18.0	13.2	54.1
1.20	2.85	6.00	4.1	5.05	15.6	19.0	13.9	56.1
			4.2	4.88	15.7	20.0	14.5	57.6

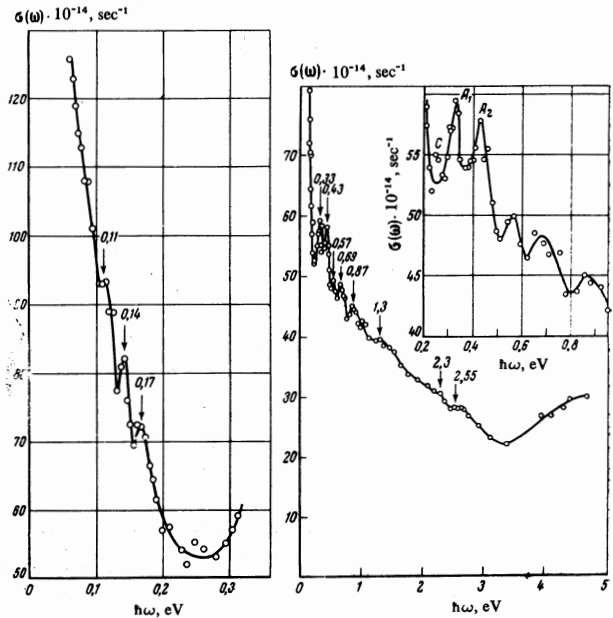FIG. 2. Optical conductivity $\sigma(\omega)$ for Ni (110).

reflection in the visible and ultraviolet regions. The measurements were performed at room temperature at steps of 1.0, 0.25, 0.1, 0.05, and 0.025 μ respectively in the spectral intervals 20−10, 10−4, 4−2, 2−1, and 1−0.4 μ. For each sample, 8−12 series of measurements were made. As expected, the values of n and k of two Ni samples $(\rho(293° K)/\rho(4.2° K) = 342)$ with (110) and (100) planes were equal within the limits of measurement errors. In a cubic crystal, in the case of the normal skin effects, the dielectric tensor ϵ_{eff} is a scalar, and the optical characteristics do not depend on the orientation of the reflecting plane. In the subsequent discussion we shall use the results obtained with Ni (110). These results are listed in Table I.

The rms error of the mean value in the wavelength region 20−1 μ was 2−3% for n and 2−4% for k. From the values of n and k we calculated the real and imaginary parts $\epsilon_1(\omega)$ and $\epsilon_2(\omega)$ of the dielectric constant of nickel and the optical conductivity $\sigma(\omega)$. The results for $\epsilon_1(\omega)$ and $\epsilon_2(\omega)$ in the visible and ultraviolet regions of the spectrum are in quantitative agreement with the data of Roberts[11] and of Ehrenreich, Philipp, and Olechna[3], pertaining to electrically polished polycrystalline samples. Exceptions are certain additional singularities in the dispersions of these quantities, which were clearly observed in the present work as a result of the good spectral resolution, and as a result of the use of perfect single-crystal samples.

DISCUSSION OF RESULTS

The complex dielectric constant of a metal $\epsilon(\omega)$ = $\epsilon_1(\omega) + i\epsilon_2(\omega)$ is the sum of the contributions of the intraband and interband electron transitions.

According to[3,12], the edge of the interband absorption in nickel is at 0.25−0.30 eV. Indeed, in the spectrum interval 20−5 μ (0.062−0.25 eV), the optical

properties of nickel are determined in the main by the intraband acceleration of the electrons, and a noticeable inclusion of the interband transitions begins with 0.25−0.30 eV (Fig. 2). At energies 0.10, 0.14, and 0.17 eV the $\sigma(\omega)$ curve also reveals bursts and deviations from monotonicity connected with the interband transitions. This allows us to conclude that the absorption edge in nickel is apparently located at an energy much lower than considered above, namely at $\hbar\omega$ $\sim$ 0.10 eV.

For nickel, as for other 3d and 4d transition metals, it is difficult to separate the intraband and interband contributions to $\sigma(\omega)$, since its optical properties in the infrared region cannot be described with a single-band model. The Argand diagram constructed from the experimental values of $\epsilon_2(\omega)\omega$ and $\epsilon_1(\omega)$ in the region 8−20 μ does not go to zero, as in the case of metals with single-band conductivity (Cu, Au), but has an intercept on the ordinate axis (Fig. 3). The reduction of the results for Ni (110) using the two-band conductivity model also encounter certain difficulties, especially in the interpretation of its optical properties in the near-infrared region. This question will be discussed in a subsequent paper.

Let us return to the interband transitions in Ni. The singularity of the absorption spectrum in the 0.3-eV region, observed in earlier experiments in the form of a step, was resolved in the present study into two bright peaks with maximum energies 0.33 and 0.43 eV (Fig. 2).
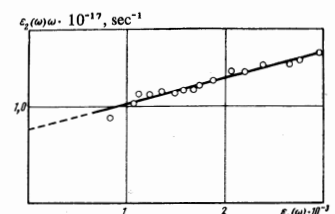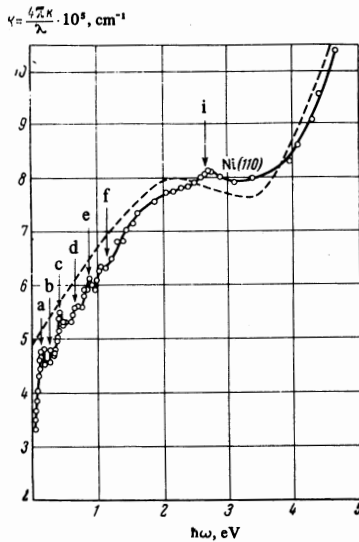

FIG. 3. Argand diagram of Ni (110).

FIG. 4. Fine structure of the absorption-coefficient curve K = $4\pi k/\lambda$: a—0.17, b—0.33, c—0.44, d—0.72, e—0.88, f—1.3, i—2.55 eV. Dashed curve—data of [3].

Conductivity bursts are also observed at 0.57, 0.69, 0.87, 1.3, 2.36, and 2.55 eV. Analogous singularities were noted on the K = $4\pi k/\lambda$ curve (Fig. 4) (λ—wavelength of the light).

Table II

Energy of singularity, eV	Measurement method	Nickel sample*
0.10	Optical	SC (110)
0.10 [8]	»	PC, MP, Annealed
0.14	»	PC (110)
0.17	»	SC (110)
0.17 [13]	»	PC, MP
0.17 [14]	Polar Kerr effect	PC, MP, Annealed
0.18 [8]	Optical	PC, MP, Annealed
0.33	»	SC (110)
0.30 [3,12]	»	PC, EP
0.25 [6]	Thermal reflection	Film
0.30 [15]	Equatorial Kerr effect	PC, EP
0.33 [14]	Polar Kerr effect	PC, MP, Annealed
0.43	Optical	SC (110)
0.44 [14]	Polar Kerr effect	PC, MP, Annealed
0.42 [8]	Optical	PC, MP, Annealed
0.40 [6]	Thermal reflection	Film
0.57	Optical	SC (110)
0.57 [8]	»	PC, MP, Film
0.69	»	SC (110)
0.72 [16,17]	Equatorial Kerr effect	SC (110)
0.71 [6]	Optical	PC, SC, Annealed
0.87	»	SC (110)
0.90 [16,17]	Equatorial Kerr effect	SC (110)
0.82 [8]	Optical	PC, MP, Annealed
1.3	»	SC (110)
1.3 [17]	Equatorial Kerr effect	SC (110)
1.3 [6]	Thermal reflection	Film
1.4 [8]	Optical	PC, EP
1.5 [8]		PC, MP, Annealed
2.17 [18]	»	PC, EP
2.25 [18]	»	PC, EP
2.36	»	SC (110)
2.34 [18]	»	PC, EP
2.30 [8]	»	PC, MP, Annealed
2.55	»	SC (110)
2.50 [17]	Equatorial Kerr effect	SC (110)
2.45 [18]	Optical	PC, EP

*SC—single crystal, PC—polycrystal, MP—mechanically polished, EP—electrically polished.

It is known that the structure on $\epsilon_2(\omega)$ and $\sigma(\omega)$ occurs for interband transitions of the electrons in the region of the critical points in k space, when $V_k E_{ll'}(\mathbf{k}) = \nabla_k E_{l'}(\mathbf{k}) - \nabla_k E_l(\mathbf{k}) = 0$, and in the case of direct transitions it characterizes definite energy gaps in the band spectrum of the metal. Similar information is also obtained from magnetooptical and temperature-modulation measurements. All the published experimental data on the energy gaps in the band spectrum of nickel, together with our data, are summarized in Table II.

In the energy region 0.3—2.5 eV, the peaks on the $\sigma(\omega)$ curve were observed at practically the same energies at which the singularities on the frequency dependence of the equatorial Kerr effect were observed in [15-17]. An exception is the singularity at $\hbar\omega$ = 0.57 eV, which was not observed in magnetooptical experiments, but was noted in optical experiments also by Sasovskaya and Noskov[8]. The energy gap determined from the thermal reflection spectra[6] is 0.25 eV. According to the data of the present paper there is no noticeable peak in this region (Fig. 2), although a certain scatter of the points, exceeding the experimental error, is observed. An energy of 0.25 eV characterizes the start of the intense interband transitions, leading to the occurrence of a sufficiently pronounced absorption band in the 0.25—0.50-eV region. The presence of low-energy gaps (0.10 and 0.17 eV) in the band spectrum of nickel was already noted earlier in optical[13] and magnetooptical[14] experiments, and quite recently by Sasovskaya and Noskov[8]. In the case of single-crystal samples, the singularities on $\sigma(\omega)$ at these energies are much more pronounced, but nonetheless low-temperature measurements are needed to confirm their existence conclusively.

In ferromagnetic nickel the two systems of bands resulting from exchange splitting are similar. They retain the general singularities of the spectrum in the nonmagnetic state. Each system of bands has a different degree of filling and, consequently, a different structure of optical interband absorption. The quantity $\sigma(\omega)$ shown in Fig. 2 is the sum of the absorption curves from bands with spins parallel (↑) and antiparallel (↓) to the magnetization. At the present time it is impossible to calculate its magnitude theoretically. Therefore a complete analysis of the optical properties of nickel in the region of interband transitions is impossible. We confine ourselves to an analysis of those peaks against the background of the continuous optical absorption the appearance of which is connected with the presence of critical points in the energy spectrum of the metal. Although a study of the optical absorption can in principle yield quantitative information concerning the energy gaps, in some cases great difficulties are encountered in the interpretation of the absorption spectrum. This pertains fully to nickel.

We consider in the present article the band structure of nickel only near the L point of the Brillouin zone. The model of the energy bands of ferromagnetic nickel proposed by Ehrenreich, Philipp and Olechna[3], assumed the following arrangement of the bands at the L point: $E(L_2'\uparrow) - E(L_{32}\uparrow) > 0$. Using a self-consistent interpolation scheme, Hodges, Ehrenreich, and Lang[19] explained many experimental data for Ni in this model. Krinchik[5], and then Hanus et al.[6] proposed a reversed
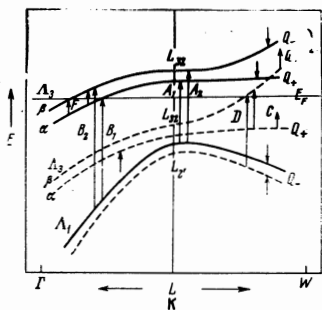
FIG. 5. Model of energy bands of ferromagnetic nickel near the point L of the Brillouin zone; k is in units of $2\pi/a$.

arrangement of these levels: $E(L_{32}\downarrow) - E(L_2'\downarrow) > 0$. Connolly's self-consistent calculation[2] for ferromagnetic nickel with potential V_4 predicts such a level arrangement for bands with spin $(\downarrow)$. Recently Zonberg[9] again analyzed in detail several qualitatively different models of the bands of ferromagnetic nickel near the L point and also reached the conclusion that the arrangement of the bands proposed in[5,6] is the most suitable for both spin subbands (Fig. 5). This model is in good agreement with galvanomagnetic data[20] which confirmed the difference in the [111] neck diameter of nickel and copper and the absence of holes near L in Ni.

Hanus, Feinleib, and Scouler[6], interpreting the spectrum of thermal reflection $\Delta R/R$, have reached the conclusion that the peak at 0.25 eV corresponds to the transition $E(Q_-\uparrow) - E(Q_+\uparrow)$, and the peak at 0.40 eV to the transitions $E(L_{32}\downarrow) - E(L_2'\downarrow)$ (Fig. 5, transitions C and A, respectively). Such an arrangement of the levels corresponds to d-exchange splitting of the bands at the point L ~ 0.4 eV. At the same time, Zonberg[9] suggests that it is possible to ascribe the singularity at 0.40 eV to the electron transition $E(Q_-\uparrow) - E(Q_+\uparrow)$ on the neck, and the singularity at 0.25 eV to the transition $E(L_{32}\downarrow) - E(L_2'\downarrow)$. This leads to a change in the position of the d-like band relative to the Fermi level and to a somewhat different estimate of the exchange splitting $(\Delta E_d = 0.57$ eV).

An examination of the singularities of optical absorption in the region of interband transitions in nickel according to the data of the present paper favors the first variant of the gap estimate. Indeed, the interband transitions begin to make a noticeable contribution to the conductivity $\sigma(\omega)$ starting with the energy 0.25 eV (Fig. 2), and lead to the occurrence of a noticeable absorption band (see the insert) in the region 0.25—0.50 eV. The specific (double) form of this band, and also its considerable intensity compared with other singularities on $\sigma(\omega)$, give grounds for assuming that its appearance in the spectrum may be connected with electron transitions between the (s-p)-like $L_2'\downarrow$ and the d-like $L_{32}\downarrow$ bands at the point L. In this case, the complex structure of the absorption band (see the insert of Fig. 2) is the result of the splitting of the L_{32} band by the spin-orbit interaction. Ascribing to the transition $E(L_{32\alpha}\downarrow) - E(L_2'\downarrow)$ an energy 0.33 eV (A_1) and to the transition $E(L_{32\beta}\downarrow) - E(L_2'\downarrow)$ an energy 0.43 eV (A_2) (Figs. 2 and 5), we find that the difference of the peak energies $\Delta E \sim 0.10$ eV corresponds to the magnitude of the spin-orbit splitting of the $L_{32}\downarrow$ level at the point L (in atomic Ni, the spin-orbit splitting is equal to 0.075 eV). The start of the intense absorption band in nickel at an energy 0.25 eV in this

model can be connected with the transition $E(Q_-\uparrow) - E(Q_+\uparrow)$ (C), i.e., with the absorption edge near L in the electron system $(\uparrow)$.

Identification of the singularities on the $\sigma(\omega)$ curve in the energy region 0.5—0.9 eV has, in our opinion, a less definite character. One can propose, for example, two variants of the gap estimate. In the first variant, assuming as in[17] that $E(\Lambda_{32\alpha}\downarrow) - E(\Lambda_1\downarrow) = 0.69$ eV, $E(\Lambda_{32\beta}\downarrow) - E(\Lambda_1\downarrow) = 0.87$ eV, and $E_{ph} - E(Q_-\uparrow) = 0.57$ eV (transitions B_1, B_2, and D on Fig. 5, respectively), we obtain the energy of the spin-orbit splitting of the edge of interband absorption in the electron system $(\downarrow)$, $\Delta E_{\alpha\beta} = 0.18$ eV. If the transition F (Fig. 5) between the split sublevels $\Lambda_{32\alpha}\downarrow$ and $\Lambda_{32\beta}\downarrow$ is allowed, then a burst should be observed on the $\sigma(\omega)$ curve in the region $\hbar\omega = 0.18$ eV. Indeed, Fig. 2 shows a burst on the experimental $\sigma(\omega)$ curve at 0.17 eV. In the second variant, the transitions indicated above can be estimated differently, namely: $E(\Lambda_{32\alpha}\downarrow) - E(\Lambda_1\downarrow) = 0.57$ eV, (B_1), $E(\Lambda_{32\beta}\downarrow) - E(\Lambda_1\downarrow) = 0.69$ eV (B_2) and $E_{ph} - E(Q_-\uparrow) = 0.87$ eV (D). In this case $\Delta E_{\alpha\beta} = 0.12$ eV (F). On the $\sigma(\omega)$ curve there is also observed a burst at the energy 0.11 eV (Fig. 2). Consequently, the presence of some singularity on $\sigma(\omega)$ at low frequencies cannot serve in this case as a criterion for a correct estimate of the gaps in the spectrum of nickel. This is due to the fact that low-energy bursts (peaks) on the $\sigma(\omega)$ curve of nickel are the result of interband transitions of the electrons not only near the point L, but also near the point $X(X_2\downarrow - X_5\downarrow,$[9]) of the Brillouin zone, and it is difficult to separate them solely on the basis of the frequency dispersion of the optical quantities. It is possible that preference should be given to the first variant of the gap estimate, for in this case the expected magnitude of the exchange splitting of the (s—p)-like level L_2' turns out to be smaller. This question calls for further study.

The interpretation of the remaining peaks on the $\sigma(\omega)$ curve for Ni (110) will not be considered in the present article. A tentative explanation of certain singularities on the curves of the optical conductivity and magnetooptical Kerr rotation, connected with the interband transitions of electrons in nickel, is already contained in[7,17,18].

Thus, the new detailed information concerning the interband transitions that has been obtained from optical measurements on single-crystal samples, supplements and confirms the earlier experimental data on the energy gaps in the band spectrum of nickel. On the whole, the optical data confirm the model representations developed in[2,5,6,9] concerning the structure of the energy bands of nickel near the L point. Further theoretical and experimental research is necessary, however, if a more unequivocal interpretation of the optical data is to be obtained.

---

[1] S. Wakoh, J. Phys. Soc. Japan, **20**, 1894, 1965.

[2] J. W. D. Connolly, Phys. Rev. **159**, 415, 1967.

[3] H. Ehrenreich, H. R. Philipp and D. J. Olechna, Phys. Rev. **131**, 2469, 1963.

[4] J. C. Phillips, Phys. Rev. **133**, A1020, 1964.

[5] G. S. Krinchik and E. A. Ganshina, Phys. Lett. **23**, 294, 1968.

[6] J. Hanus, J. Feinleib and W. J. Scouler, Phys. Rev. Lett. **19**, 16, 1967; J. Appl. Phys. **39**, 1272, 1968.

[7] M. Shiga and G. P. Pells, Solid State Phys. **2**, 1847, 1969.

[8] I. I. Sasovskaya and M. M. Noskov, Fiz. Met. Metallov. (1971) (in press).

[9] E. J. Zonberg, Phys. Rev. B1, 244, 1970.

[10] J. R. Beattie, Phil. Mag. **46**, 235, 1955.

[11] S. Roberts, Phys. Rev. **114**, 104, 1959.

[12] J. R. Beattie and G. K. Conn, Phil. Mag. **46**, 1002, 1955.

[13] G. A. Bolotin, M. M. Kirillova, L. V. Nomerovannaya, and M. M. Noskov, Fiz. Met. Metallov. **23**, 463 (1967).

[14] L. A. Afanas'eva, G. A. Bolotin, and M. M. Noskov, ibid. **22**, 828 (1966).

[15] G. S. Krinchik and G. M. Nurmukhamedov, Zh. Eksp. Teor. Fiz. **48**, 34 (1965) [Sov. Phys.-JETP **21**, 22 (1965)].

[16] G. S. Krinchik, V. S. Gushchin and E. A. Gan'shina, ZhETF Pis. Red. **8**, 53 (1968) [JETP Lett. **8**, 31 (1968)].

[17] G. S. Krinchik and V. S. Gushchin, ibid. **56**, 1833 (1969) [**29**, 984 (1969)].

[18] M. Ph. Stoll, Sol. State Commun. **8**, 1207, 1970.

[19] L. Hodges, H. Ehrenreich and N. D. Lang, Phys. Rev. **152**, 505, 1966.

[20] A. S. Joseph and A. C. Thorsen, Phys. Rev. Lett. **11**, 556, 1963; D. C. Tsui and R. W. Stark, Phys. Rev. Letters **17**, 871, 1966; R. W. Stark and D. C. Tsui, J. Appl. Phys. **39**, 1056, 1968.

Translated by J. G. Adashko

34